Supplementary materials for "On-chip all-optical nonreciprocal device for short-pulse isolator based on free carrier dispersion effect"

Qilin Hong[1†], Wei Xu[1,3†], Gongyu Xia[1†], Wen Chen[4], Qilin Zheng[2], Jiacheng Liu[1], Pingyu Zhu[2], Jianfa Zhang[1], Ping Xu[2,5*], Zhihong Zhu[1*]

[1*]College of Advanced Interdisciplinary Studies & Hunan Provincial Key Laboratory of Novel Nano Optoelectronic Information Materials and Devices, National University of Defense Technology, Changsha, 410073, China.

[2*]Institute for Quantum Information and State Key Laboratory of High-Performance Computing, College of Computer Science and Technology, National University of Defense Technology, Changsha, 410073, China.

[3]Nanhu Laser Laboratory, National University of Defense Technology, Changsha, 410073, China.

[4]College of Meteorology and Oceanography, National University of Defense Technology, Changsha, 410073, China.

[5]Hefei National Laboratory, Hefei, 230088, China.

*Corresponding author(s). E-mail(s): pingxu520@nju.edu.cn; zzhwcx@163.com;

†These authors contributed equally to this work.

S1 Linear response of the structure

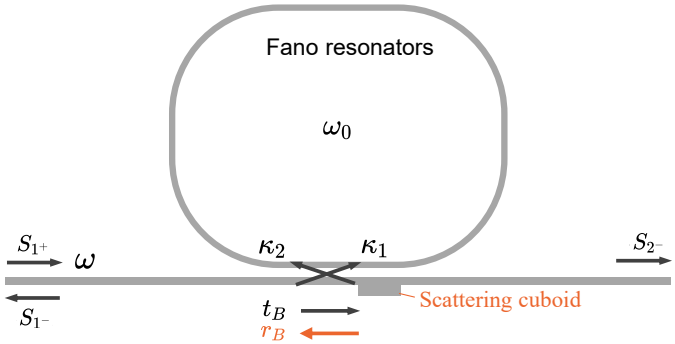

Fig. S1 The schematic of the proposed structure

According to the coupled-mode theory[1], for the structure of a double-port single-resonance cavity, considering the situation of nonlinear response, and single-port input, the amplitude $a(\omega, t)$ could be written as

$$\frac{da}{dt} = \left(-\gamma_{\text{in}} - \gamma_A - j(\omega_0 + \Delta\omega)\right) a + \sqrt{2\gamma_1} e^{j\theta_1} S_{1^+} \tag{S1}$$

where $\Delta\omega$ is the frequency shift caused by nonlinear effects and is 0 for the linear response. ω is the incident frequency, ω_0 is the intrinsic frequency of the cavity, $\gamma_{\text{in}} = \gamma_1 + \gamma_2$ and γ_1, γ_2 are the decay rates towards two ports of the bus waveguide. γ_A is the intrinsic loss rate of the cavity, S_{1^+} are the amplitudes of the input wave. κ_1 and κ_2 are the complex coupling rates from the bus waveguide to the cavity, respectively.

Define the direct coupling matrix $\boldsymbol{C}$ for the two ports as

$$\boldsymbol{C} = e^{j\phi} \begin{bmatrix} r_B & jt_B \\ jt_B & r_B \end{bmatrix} \tag{S2}$$

where r_B, t_B and ϕ are all real numbers. The energy conservation requires $r_B^2 + t_B^2 = 1$. Noting that the 'ϕ' item could be 0 in the case of choosing suitable reference plane.

The output waves for another port could be written as

$$S_{2^-} = e^{j\phi} \cdot jt_B S_{1^+} + \sqrt{2\gamma_2} e^{j\theta_2} a \tag{S3}$$

Constrained by the time-reversal symmetry[1], we could derive $\kappa_1 = \sqrt{2\gamma_1} e^{j\theta_1}$, $\kappa_2 = \sqrt{2\gamma_2} e^{j\theta_2}$ and

$$\boldsymbol{C} \begin{bmatrix} \kappa_1^* \\ \kappa_2^* \end{bmatrix} = - \begin{bmatrix} \kappa_1 \\ \kappa_2 \end{bmatrix}. \tag{S4}$$

In this model, we only discuss the situation of steady-state and single-frequency excitation, so $da/dt = -j\omega a$.

Combining equ. S1, equ. S3 and equ. S4, the transmission of the structure can be written as

$$T = \left|\frac{S_{2-}}{S_{1+}}\right|^2 = \left|jt_B - \frac{2\left(r_B\sqrt{\gamma_1\gamma_2}e^{j(\theta_2-\theta_1)} + jt_B\gamma_2\right)}{j\left(\omega_0 + \Delta\omega - \omega\right) + \gamma_t}\right|^2 \tag{S5}$$

Herein, $\gamma_t = \gamma_{\text{in}} + \gamma_A$ is the total loss.

Then we discuss the conditions of the phase items θ_1 and θ_2. From equ. S4, we have

$$\begin{cases} r_B e^{-j\theta_1} + jt_B\sqrt{\frac{\gamma_2}{\gamma_1}}e^{-j\theta_2} = -e^{j\theta_1 - j\phi} \\ jt_B e^{-j\theta_1} + r_B\sqrt{\frac{\gamma_2}{\gamma_1}}e^{-j\theta_2} = -\sqrt{\frac{\gamma_2}{\gamma_1}}e^{j\theta_2 - j\phi} \end{cases} \tag{S6}$$

Multiply $e^{j\theta_1}$ for both equations, we have

$$e^{j(\theta_2-\theta_1)} = \mp jt_B\sqrt{\frac{\gamma_2}{\gamma_1}} \cdot \frac{1}{r_B + e^{j(2\theta_1-\phi)}} \tag{S7}$$

$$jt_B + r_B\sqrt{\frac{\gamma_2}{\gamma_1}}e^{-j(\theta_2-\theta_1)} = -\sqrt{\frac{\gamma_2}{\gamma_1}}e^{j(\theta_2-\theta_1)} \cdot e^{j(2\theta_1-\phi)} \tag{S8}$$

where the '$\mp$' sign determines the shape of the Fano resonance (transmission peaks followed by dips or vice versa as the wavelength increases along the x-axis).

Substituting equ. S7 into equ. S8 and expanding it using Euler's formula, we have

$$\begin{aligned} &t_B^2\left[r_B + \cos(2\theta_1 - \phi) + j\sin(2\theta_1 - \phi)\right] + r_B\left[(r_B + \cos(2\theta_1 - \phi) + j\sin(2\theta_1 - \phi)\right]^2 \\ &= t_B^2\frac{\gamma_2}{\gamma_1}\left[\cos(2\theta_1 - \phi) + j\sin(2\theta_1 - \phi)\right] \end{aligned} \tag{S9}$$

Since all the variables in the expression are real except for j, the expression can be expanded and rearranged separately based on their real and imaginary parts. It is easy to derive

$$\cos(2\theta_1 - \phi) = \frac{t_B^2}{2r_B}\left(\frac{\gamma_2}{\gamma_1} - 1\right) - r_B \tag{S10}$$

Therefore, equ. S7 and equ. S10 are the conditions that phase items θ_1 and θ_2 need to satisfy.

With equ. S5, euq. S7 and equ. S10, one could plot the transmittance versus wavelength of the structure with proper parameters.

S2 Nonlinear response of the structure

In order to theoretically obtain the transmission spectra at different input powers, equ. S5 also needs to know the nonlinear frequency shift at different powers. With a monochromatic input, equ. S1 and the complex conjugate of equ. S1 are given as

$$\begin{aligned} -\sqrt{2\gamma_1}e^{j\theta_1}S_{1+} &= (-\gamma_t - j(\omega_0 + \Delta\omega - \omega))a \\ -\sqrt{2\gamma_1}e^{-j\theta_1}S^*_{1+} &= (-\gamma_t + j(\omega_0 + \Delta\omega - \omega))a^* \end{aligned} \tag{S11}$$

Multiply them

$$2\gamma_1 P_{\text{in}} = \left(\gamma_t^2 + (\omega_0 + \Delta\omega - \omega)^2\right)|a|^2 \tag{S12}$$

Here, $P_{\text{in}} = |S_{1+}|^2$ represents the input power on chip. Therefore, we just need to solve equ. S12 to obtain the frequency shift for different powers.

Next, we analyze the item of nonlinear frequency shift $\Delta\omega$.

For silicon, as discussed in the manuscript, the lack of centrosymmetry in its structure results in the absence of second-order nonlinear effects. Therefore, we mainly focus on the third-order nonlinear effects of silicon. The third-order nonlinearity of silicon includes the Kerr effect, two-photon absorption (TPA), free-carrier effect (FCE), and the thermo-optic effect (TOE) caused by TPA and FCA[2, 3].

According to the model in reference [4], the nonlinear frequency shift $\Delta\omega$ could be written as

$$\Delta\omega = \Delta\omega_{\text{NL}}(U) + j\tau_{\text{NL}}^{-1}(U) \tag{S13}$$

$$\Delta\omega_{\text{NL}}(U) = \Delta\omega_{\text{Kerr}}\left(\frac{U}{V^{(3)}}\right) + \Delta\omega_{\text{TOE}}\left(\frac{U^2}{V_{\text{TOE}}^2}\right) + \Delta\omega_{\text{FCD}}\left(\frac{U^2}{V_{\text{FCE}}^2}\right) \tag{S14}$$

Herein, $U(t) = |a|^2$ represents the intracavity energy, V is the mode volume. The subscript 'TOE' denotes the thermo-optic effect. 'FCD' denotes the free-carrier dispersion effect.

In this supplementary material, we do not intend to derive the expressions of nonlinear frequency shift again, but rather to introduce the approach and specific expressions in the reference[4]. For specific derivation details, please refer to the original text.

The core of the approach is regarding nonlinear effects as perturbations to linear system. Starting from the Maxwell's equations, one can obtain that for a linear system, the electric field inside the micro-ring satisfies

$$\nabla \times (\nabla \times \mathbf{E}_0(\mathbf{r}, t)) = \omega_0^2 \mu_0 \varepsilon(\mathbf{r}) \mathbf{E}_0(\mathbf{r}, t) \tag{S15}$$

where $\varepsilon(\mathbf{r})$ denotes the linear permittivity and μ_0 denotes the vacuum permeability.

Considering the nonlinearity, the polarization will change the refractive index of the microcavity and shifts its intrinsic resonance to $\omega_0^{'}$

$$\nabla \times (\nabla \times \mathbf{E}(\mathbf{r}, t)) = \omega_0'^2 \mu_0 \varepsilon(\mathbf{r}) \mathbf{E}(\mathbf{r}, t) + \omega_0'^2 \mu_0 \mathbf{P}_{\text{NL}}(\mathbf{r}, t) \tag{S16}$$

Herein, only the harmonic field at $\omega_0^{'}$ are considered. Expanding the 't' item of the electric field and polarization in the form of Fourier expansions

$$\begin{aligned}\mathbf{E}(\mathbf{r},t) &= \frac{1}{2}\mathbf{E}(\mathbf{r})e^{-j\omega_0^{'}t} + \text{ c.c.} \\ \mathbf{P}_{\mathrm{NL}}(\mathbf{r},t) &= \frac{1}{2}\mathbf{P}_{\mathrm{NL}}(\mathbf{r})e^{-j\omega_0^{'}t} + \text{ c.c.}\end{aligned} \tag{S17}$$

Given that the nonlinear polarization is typically weak, it can be regarded as a perturbation to the linear cavity mode. Therefore, the electric field and frequency can be approximated using Taylor expansions to the first order, as $\mathbf{E}(\mathbf{r}) \approx \mathbf{E}_0(\mathbf{r}) + \Delta\mathbf{E}$ and $\omega_0' \approx \omega_0 + \Delta\omega$. Substituting these approximations into equ. S16, the nonlinear frequency shift can be expressed as[5]

$$\frac{\Delta\omega}{\omega_0} \approx -\frac{1}{2}\frac{\iiint dV\left\{\mathbf{E}_0^*(\mathbf{r})\cdot\mathbf{P}_{\mathrm{NL}}(\mathbf{r})\right\}}{\iiint dV\left\{\varepsilon(\mathbf{r})\mathbf{E}_0^*(\mathbf{r})\cdot\mathbf{E}_0(\mathbf{r})\right\}} \tag{S18}$$

Therefore, when $\mathbf{P}_{\mathrm{NL}}(\mathbf{r})$ is written as a specific function of the electric field for different nonlinear effects, the analytical expression for $\Delta\omega$ caused by different nonlinear effects can be determined through equ. S18, and the total frequency shift is the sum of the frequency shifts caused by various nonlinear effects.

The nonlinear effects we discuss are mainly Kerr effect, FCD effect and TOE effect caused by TPA. The expressions are listed as follows

$$\Delta\omega_{\mathrm{Kerr}} \approx -\frac{cn_2\omega_0 U}{V^{(3)}} \tag{S19}$$

$$\Delta\omega_{\mathrm{FCD}} \approx \frac{f\tau_{\mathrm{c}}\beta c^2}{2\hbar}\frac{U^2}{V_{\mathrm{FCE}}^2} \tag{S20}$$

$$\Delta\omega_{\mathrm{TOE}} \approx -\omega_0 c^2\beta\frac{\kappa_\theta\tau_\theta}{C\rho}\frac{U^2}{V_{\mathrm{FCE}}^2} \tag{S21}$$

where $U \approx \iiint dV(\varepsilon\left|\mathbf{E}_0\right|^2)/2$, c is light speed in vacuum, $n_2 = 4.0\times10^{-18}$ m^2/W denotes Kerr coefficient of silicon, $\beta = 8.0\times10^{-12}$ m/W denotes TPA coefficient[6]. $\tau_c = 0.5$ ns is free carrier recombination time. $\tau_\theta = 1$ μs is thermal dissipation time. $\kappa_\theta = 1.86\times10^{-4}$ K^{-1} is thermo-optic coefficient. $C = 705$ J/(kg $\cdot$ K) is thermal capacity of silicon. $\rho = 2.3\times10^3$ kg/m^3 is mass density of silicon. $f = (8.8\times10^{-6}N + 1.3N^{0.8})\times10^{-22}/N$, and N is the local electron or hole density[7]. $V^{(3)}$ denotes the mode volume of Kerr effect and the expression is

$$V^{(3)} = \frac{3}{\varepsilon_0}\frac{\left(\iiint dV\varepsilon\left|\mathbf{E}_0\right|^2\right)^2}{\iiint_{\mathrm{Si}} dV\varepsilon\left\{(3-\eta)\left|\mathbf{E}_0\right|^4 + \eta\left(\mathbf{E}_0^*\cdot\mathbf{E}_0^*\right)\left(\mathbf{E}_0\cdot\mathbf{E}_0\right)\right\}} \tag{S22}$$

V_{FCE} is the mode volume of free carrier effect and the expression is

$$V_{\mathrm{FCE}} = \sqrt{\frac{3}{\varepsilon_0^2} \frac{\left(\iiint dV\varepsilon \left|\mathbf{E}_0\right|^2\right)^3}{\iiint_{\mathrm{Si}} dV\varepsilon \left|\mathbf{E}_0\right|^2 \left\{(3-\eta)\left|\mathbf{E}_0\right|^4 + \eta\left(\mathbf{E}_0^* \cdot \mathbf{E}_0^*\right)\left(\mathbf{E}_0 \cdot \mathbf{E}_0\right)\right\}}} \tag{S23}$$

S3 Numerical solving of the nonlinear model

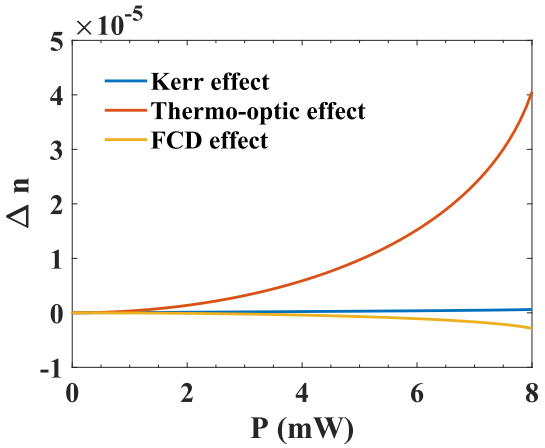

Fig. S2 Index changes versus on-chip power with different nonlinear effects.

To analyze the contributions of different nonlinear effects to the total third-order nonlinear effect, we then solve the model in Sec. S2.

By substituting equ. S19 - equ. S21 into equ. S12 and neglecting the loss resulted from nonlinear effects, we can obtain a fifth-order single-variable equation for intracavity energy U with respect to the given on-chip power P. Using MATLAB to solve this equation for real solutions, the function of U with respect to power P is solved. Substituting the obtained U back into equ. S19 - equ. S21 and use

$$\frac{\Delta\omega}{\omega} \approx -\frac{\Delta n}{n} \tag{S24}$$

one can obtain specific values of the frequency-shift capability of different nonlinear effects.

Apparently, as shown in the Fig. S2, among the various nonlinear effects in silicon, the dominant effect is the thermo-optic effect caused by TPA, which is approximately an order of magnitude larger than the FCD. The Kerr effect is very weak and almost negligible in the presence of other effects. So we can derive that, under the condition of c.w. laser, the thermo-optic effect will overcome the FCD effect and lead to the redshift of the wavelength. While with the pulse-laser input and the pulse width is too short to accumulate the heat, the main nonlinear effect will be FCD effect and cause blueshift of the wavelength correspondingly.

S4 Analytical solution of NTR

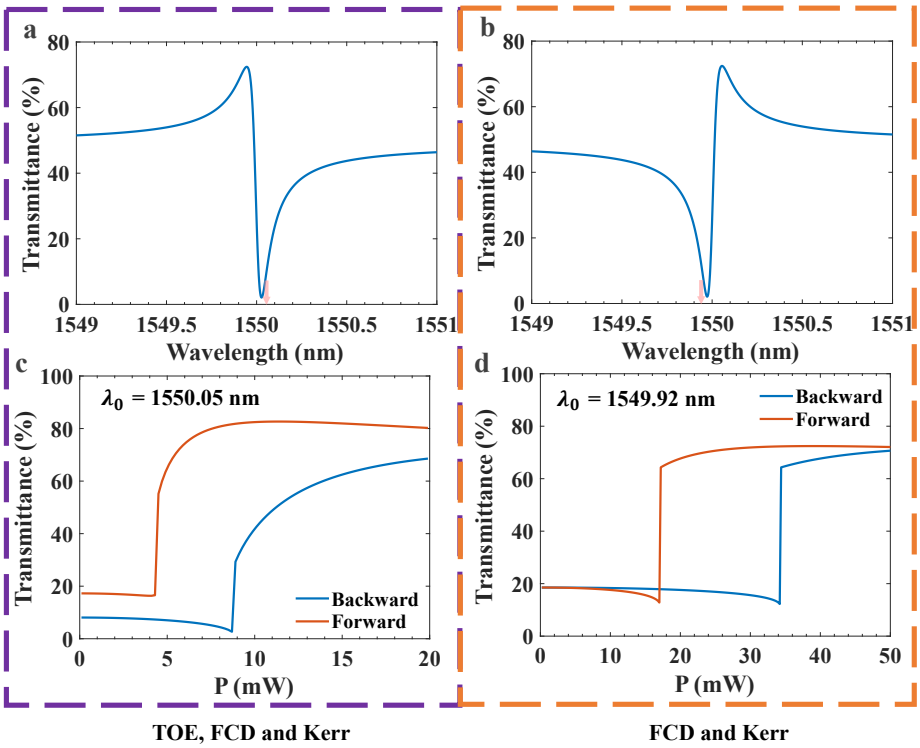

Fig. S3 **a-b** Theoretical transmission spectral of a Fano resonator with different phases. **c-d** NTR versus on-chip power for a monochromatic input. **(c)** corresponds to **(a)** at a fixed wavelength of 1550.05 nm (the pink arrow in **(a)**), taking into account the effects of TOE, FCD and Kerr collectively. The dominant nonlinear effect leads the resonant wavelength in cavity shifting towards longer wavelengths. **(d)** corresponds to **(b)** at a fixed wavelength of 1549.92 nm (the pink arrow in **(b)**), taking into account the effects of FCD and Kerr while the TOE is neglected. The dominant nonlinear effect leads to the resonant wavelength in cavity shifting towards shorter wavelengths.

Based on the model in Sec. S1 and Sec. S2, we can also show the NTR of the structure theoretically.

Using equ. S5, the transmission spectrum of the resonant structure in linear response can be obtained. Here, we set the intrinsic Q_i value to 80000, the total Q_t value to 20000, $\gamma_2/\gamma_1 = 2$, $\gamma_t = \omega_0/(2Q_t)$, $\omega_0 = 2\pi c/\lambda_0$. $\lambda_0 = 1550$ nm is the central wavelength. Set the background direct transmission coefficient to $t_B = 0.7$. Fig. S3a and Fig. S3b show the resulting Fano line shapes under these parameters, where the former corresponds to taking the negative sign in equ. S7, and the latter corresponds to taking the positive sign.

Furthermore, by adding the nonlinear shift $\Delta\omega$ into equ. S5, the transmittance versus on-chip power could be plotted, as shown in Fig. S3c and Fig. S3d

S5 Solution for bidirectional pulse-laser input simultaneously

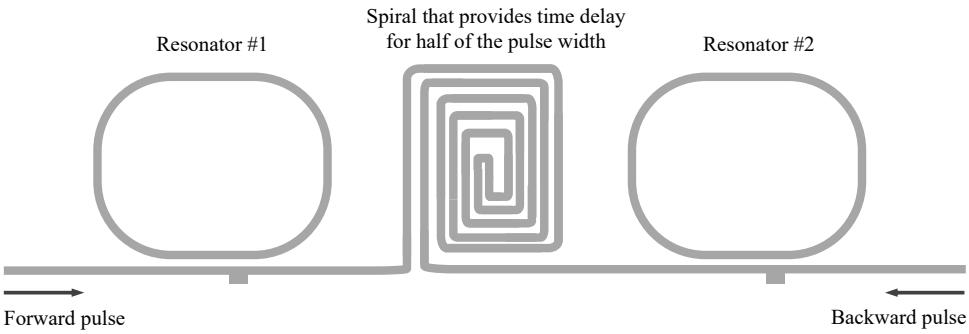

Fig. S4 Cascaded resonator and spiral structure for bidirectional pulse input at the same time.

In the manuscript, there is an 84 ns delay between forward and backward light. Here we design a double isolating structure and a spiral in the middle to achieve isolation for simultaneous pulse-light input, as shown in Fig. S4. The time delay caused by the spiral structure should be equal to or greater than half of the pulse width. For example, for the 1 ns pulse width used in the manuscript, spiral should be longer than

$$0.5 \times 10^{-9} \times \frac{3 \times 10^{8}}{3.46} \approx 43.4 \text{ mm}$$

.

Here is a simple timing analysis: #1 and #2 represent cascaded proposed structures. Considering at time t_1, forward and backward light simultaneously arrive at resonator #2. At this moment, resonator #2 fails to isolate, allowing the backward light to pass through resonator #2 and continue propagating. Half a pulse width later, due to the presence of the spiral, the forward pulsed light has completely passed through resonator #1, while the backward pulsed light has just reached resonator #1. At this moment, the backward pulsed light will be isolated by resonator #1. Therefore, from the whole system, the pulse could be input from two ports simultaneously.

References

[1] Fan, S., Suh, W. & Joannopoulos, J. D. Temporal coupled-mode theory for the fano resonance in optical resonators. *JOSA A* **20**, 569–572 (2003).

[2] Leuthold, J., Koos, C. & Freude, W. Nonlinear silicon photonics. *Nature Photonics* **4**, 535–544 (2010).

[3] Osgood, J., R. M. *et al.* Engineering nonlinearities in nanoscale optical systems: physics and applications in dispersion-engineered silicon nanophotonic wires. *Advances in Optics and Photonics* **1**, 162 (2009).

[4] Wang, J. *et al.* A theoretical model for an optical diode built with nonlinear silicon microrings. *Journal of Lightwave Technology* **31**, 313–321 (2013).

[5] Soljacic, M., Ibanescu, M., Johnson, S. G., Fink, Y. & Joannopoulos, J. D. Optimal bistable switching in nonlinear photonic crystals. *Physical Review E* **66**, 055601 (2002).

[6] Dinu, M., Quochi, F. & Garcia, H. Third-order nonlinearities in silicon at telecom wavelengths. *Applied Physics Letters* **82**, 2954–2956 (2003).

[7] Soref, R. & Bennett, B. Electrooptical effects in silicon. *IEEE Journal of Quantum Electronics* **23**, 123–129 (1987).